

Optimization of the electrochemical synthesis of silver nanoparticles in poly(vinyl alcohol) colloid solutions

R. Surudži¹, A. Jankovi¹, M. Vukašinovi -Sekuli¹, A. Peri -Gruji¹, K. Y. Rhee², V. Miškovi - Stankovi^{1,2*}

¹Faculty of Technology and Metallurgy, University of Belgrade, Karnegijeva 4, 11 000 Belgrade, Serbia,

²Department of Mechanical Engineering, College of Engineering, Kyung Hee University, Yongin, 446-701, Korea

Received November 4, 2016 Revised March 6, 2017

This work focuses on the optimization of electrochemical synthesis of silver nanoparticles in poly(vinyl alcohol) colloid solutions, films and hydrogel discs with the ability for immobilization of silver nanoparticles and their progressive release, as a new, prospective generation of medical wound dressings. Incorporation of silver nanoparticles into polyvinyl alcohol and polyvinyl alcohol/graphene matrices, with the aim to determine the effect of silver and graphene, was achieved by the electrochemical synthesis at different values of constant current density between 10 and 40 mA cm⁻² and for different time between 10 and 75 min, followed by drying (to obtain films) or freezing-thawing method (to obtain hydrogels). Synthesized nanocomposites were characterized by UV-Visible spectroscopy (UV-Vis), transmission electron microscopy (TEM), cyclic voltammetry (CV), Fourier transform infrared spectroscopy (FT-IR), Raman spectroscopy and atomic absorption spectroscopy (AAS). Additionally, antibacterial activity of thus prepared samples was evaluated against pathogenic bacteria strains *Staphylococcus aureus* and *Escherichia coli* using agar diffusion test. The results indicated that both silver/polyvinyl alcohol and silver polyvinyl alcohol/graphene nanocomposites are excellent candidates for soft tissue implants and wound dressings.

Key words: electrochemical synthesis, silver nanoparticles, graphene, poly(vinyl alcohol).

INTRODUCTION

Poly(vinyl alcohol) (PVA) is widely used in biomedical field [1-4] due to its excellent mechanical strength, low toxicity and high biocompatibility [5,6]. PVA hydrogels are three-dimensional network structures generated through crosslinking of linear polymer materials that do not dissolve in water at a physiological temperature or pH, but swell considerably in an aqueous medium [3,7,8]. PVA hydrogels have a wide range of applications in the medical and pharmaceutical areas since they can absorb exudates from wounds and consequently promote the wound healing [3,8,9].

Graphene (Gr), a single layered two-dimensional atomic carbon sheet, has drawn much attention for scientific interests and industrial applications because it has outstanding mechanical, thermal and electrical properties [10-13]. Therefore, it has great potential for use in a wide range of possible applications such as sensors, for energy storage, in nanoelectronics and polymer nanocomposites [10,14]. Due to its high mechanical strength and Young's modulus, graphene is considered as one of the most promising candidates

for the reinforcement and functionalization of polymers. The incorporation of very small amounts of graphene could significantly improve the mechanical properties [15-20].

Silver as a metal and in its ionic form, exhibits strong cytotoxicity towards a broad range of microorganisms and its use as an antibacterial agent is well known [21]. Silver nanoparticles (AgNPs) are well established antibacterial agents against the bacteria commonly present in the burn wound. Due to the excellent bactericidal property, numerous silver containing materials have been used for the treatment of burn wounds [22-24]. The stabilization of silver nanoparticles using polymer is a method of steric stabilization in solution achieved by binding the polymer molecules with long alkyl chains to the particle surface [25,26]. PVA exhibits capping ability with AgNPs [27,28]. Loading silver nanoparticles into the PVA matrix could enhance the wound healing property of the hydrogel by keeping the environment moisturized as well as by killing the bacteria on site, and thus, avoiding infection of the wound [27].

In this work silver nanoparticles were electrochemically synthesized in PVA solution at different values of constant current density between 10 and 40 mA cm⁻² and for different time periods between 10 and 75 min, in order to determine the

To whom all correspondence should be sent:
E-mail: vesna@tmf.bg.ac.rs

optimal synthesis parameters, and to compare Ag/PVA colloid dispersion obtained at optimal parameters with previously synthesized Ag/PVA/Gr colloid dispersion at constant current density of 40 mA cm⁻² and time of 30 min. The goal of our research was a thorough analysis of the effect of the current density and time of electrochemical synthesis on the amount and size of AgNPs, as well as the interaction between silver nanoparticles, PVA and graphene. UV-Vis, FT-IR and cyclic voltammetry were used for verification of the optimized parameters. Prepared Ag/PVA and Ag/PVA/Gr colloid solutions, films and hydrogel discs are intended for future medical applications as wound dressings, soft tissue implants or could serve as drug carriers.

EXPERIMENTAL

Materials and methods

The following chemicals were utilized in this work: fully hydrolyzed PVA powder ("hot soluble", Mw = 70000-100000 g mol⁻¹ Sigma, St. Louis, MO, USA), AgNO₃ (M. P. Hemija, Belgrade, Serbia), KNO₃ (Centrohem, Stara Pazova, Serbia), and graphene powders (Graphene Supermarket, Calverton, NY, USA). In all experiments ultra-pure water from a Milli-Q system (Millipore, Billerica, MA, USA) was used, as well as N₂ gas of high purity (99.5%, Messer Tehnogas a.d., Belgrade, Serbia).

Electrochemical synthesis of silver nanoparticles in PVA and PVA/Gr matrices

In order to prepare Ag/PVA and Ag/PVA/Gr colloid dispersions, films and hydrogel discs, the following procedure was applied [18,19]. PVA powder was first dissolved in hot water (90°C), and after cooling of the solution at room temperature, it was mixed with KNO₃ and AgNO₃ to obtain a solution with a final concentration of 10 wt.% PVA, 0.1 M KNO₃, and 3.9 mM AgNO₃. To prepare Ag/PVA/Gr, graphene was added to dissolved PVA under vigorous stirring. After the solution was cooled to room temperature and sonicated, KNO₃ and AgNO₃ were added to obtain a final concentration of 10 wt.% PVA, 0.01 wt.% Gr, 0.1 M KNO₃, and 3.9 mM AgNO₃. Electrochemical reduction of silver ions was performed galvanostatically using a Reference 600 potentiostat/galvanostat/ZRA (Gamry Instruments, Warminster, PA, USA) in an electrochemical cell containing 50 cm³ of PVA solution or PVA/Gr dispersion. Two platinum electrodes were employed as working and counter electrodes, and a saturated calomel electrode (SCE) was used as a

reference electrode. The applied current density was varied from 10 to 40 mA cm⁻², while reaction time was between 10 and 75 min. Synthesis was performed in N₂ atmosphere under continuous stirring.

PVA solution, PVA/Gr, Ag/PVA and Ag/PVA/Gr colloid dispersions were then poured slowly into a Teflon dish. The solvent was then allowed to evaporate at room temperature for 3 days, and the samples were further dried at 60°C for 2 days to completely remove the remaining water to yield PVA, PVA/Gr, Ag/PVA and Ag/PVA/Gr films by casting. Films with an average thickness of approximately 70 μm were peeled off the substrate for testing.

In order to obtain hydrogel discs (diameter, d=10 mm) the PVA solution, PVA/Gr, Ag/PVA and Ag/PVA/Gr colloid dispersions were subjected to five cycles of successive freezing and thawing (one cycle involved freezing for 16 h at -18°C and thawing for 8 h at 4°C).

Methods of characterization

UV-Visible spectroscopy (UV-Vis). UV-Vis spectra of Ag/PVA and Ag/PVA/Gr colloid dispersions were recorded by a UV-3100 spectrophotometer (MAPADA, Japan) in the wavelength range between 200 and 1000 nm.

Transmission electron microscopy (TEM). Transmission electron microscopy of Ag/PVA and Ag/PVA/Gr colloid dispersions was performed by 100 CX Electron Microscope (JEOL Ltd., Tokyo, Japan) operated at 100 kV, in order to examine the size and shape of Ag nanoparticles. Samples for TEM analysis were prepared by deposition of diluted Ag/PVA colloid dispersions (1:4) on C-coated Cu grids (SPI Supplies/Structure Probe Inc., West Chester, PA, USA).

Cyclic voltammetry (CV). CV measurements of the Pt electrode in Ag/PVA and Ag/PVA/Gr colloid dispersions were performed using two platinum electrodes as working and counter electrodes, and saturated calomel electrode (SCE) as a reference electrode, using a Reference 600 potentiostat/galvanostat ZRA (Gamry Instruments) at a scan rate of 50 mV s⁻¹ in the potential region from -1 to 1 V vs. SCE, starting from the open circuit potential, E_{ocp}. All potentials are reported versus the SCE, and stationary voltammograms are shown.

Fourier transform infrared spectroscopy (FT-IR). The IR spectra were recorded on PVA, Ag/PVA and Ag/PVA/Gr thin films obtained by evaporating the solvent from PVA solution, Ag/PVA and Ag/PVA/Gr colloid dispersions. The instrument used was Thermoelectron corporation

Nicolet 380 FT-IR spectrophotometer, operating in ATR mode.

Antibacterial activity test. The antibacterial activity of the PVA, PVA/Gr, Ag/PVA and Ag/PVA/Gr hydrogel discs containing a maximum of 1 mM AgNPs was tested against the Gram-positive pathogenic bacterium *Staphylococcus aureus* TL (culture collection-FTM, University of Belgrade, Serbia) and the Gram-negative bacterium *Escherichia coli* (ATCC 25922) by the agar diffusion method. Inoculums of the two microorganisms were prepared from fresh overnight LB broth (Lennox) (10 g/L tryptone, 5 g/L yeast extract, 5 g/L NaCl) cultures incubated at 37°C. The agar diffusion test was performed in LB broth containing 0.7 wt% agar. The diffusion technique was conducted by pouring media into Petri dishes to form 4 mm thick layers and adding a dense inoculum of the targeted bacteria to obtain semiconfluent growth. Petri plates were left for 15 min to dry in air and subsequently Ag/PVA or Ag/PVA/Gr hydrogels discs were placed on the agar surface and the plates were incubated for 24 h at 37°C. The width of the zone of inhibition (mm) was then measured.

Silver release monitoring. Release of silver from the Ag/PVA and Ag/PVA/Gr hydrogel discs was investigated at $37 \pm 1^\circ\text{C}$ in simulated body fluid (SBF, pH 7.4) containing 0.39 mM KH_2PO_4 + 0.61 mM K_2HPO_4 . The SBF was Cl-ion free to avoid eventual AgCl_2 precipitation. Ag/PVA and Ag/PVA/Gr hydrogel discs ($d \approx 10$ mm, ≈ 5 mm) were placed in 10 ml of SBF, which was changed periodically: every day for the first 7 days, and after that on days 10, 14, 24, and 28. Atomic absorption spectrometer (PYU UNICAM SP9, Philips, Amsterdam, Netherlands) was used to measure the silver content in the solution. Total content of silver inside the hydrogels was determined by treatment with HNO_3 (1:1 v/v), which induced oxidation of all AgNPs into Ag^+ . Experiments were performed in triplicate.

RESULTS AND DISCUSSION

UV-vis spectroscopy

UV-Vis spectroscopy was employed to monitor the silver nanoparticles formation. Nano-sized silver exhibits a strong absorption due to the collective oscillation of the conduction electrons, after appropriate excitement by suitable radiation. This phenomenon is known as a localized surface plasmon resonance (LSPR), highly dependent on the size and shape of nanoparticles [28].

Fig. 1 (a) shows the absorption spectra of pure 10 wt. % PVA solution and Ag/PVA colloid dispersions obtained at different values of current density 10, 15, 25, 40 mA cm^{-2} , and the duration of synthesis set for 10 min. PVA spectrum did not exhibit the absorbance peak in the examined wavelength range. All Ag/PVA colloid dispersions exhibited absorption spectra with two bands peaking at approximately 400 nm and 650 nm. The absorption peaks at 423, 422, 427, 423 nm for 10, 15, 25, 40 mA cm^{-2} current density, respectively, confirmed the formation of silver nanoparticles [26,28]. As the current density increased, the maximum of the absorption peak also increased, suggesting that a higher concentration of silver nanoparticles was achieved at higher current densities, since the silver nanoparticle concentration is proportional to the absorbance intensity [29, 30].

The absorption band peaking at nearly 650 nm can be explained by aggregation or agglomeration of silver nanoparticles present in the colloid solution [29, 31].

Fig. 1 (b) shows the absorption spectra of pure 10 wt. % PVA solution and Ag/PVA colloid dispersions for different time periods of synthesis 10, 30, 45, 75 min, respectively, at current density of 40 mA cm^{-2} . The increase in time of synthesis (10, 30, 45 min) increased the maximum of absorption peak at approx. 420 nm, indicating the higher concentration of silver nanoparticles, up to 75 min of synthesis time, when maximum of absorption peak decreased. In addition, the maximum of absorption peak at around 650 nm also increased, so it can be concluded that aggregation or agglomeration of silver nanoparticles is more pronounced for longer time of the synthesis. Based on these data, optimal synthesis parameters are set at current density of 40 mA cm^{-2} and time of 30 min. Ag/PVA/Gr colloid dispersion was obtained under the same conditions [18]. Since the concentration of AgNPs is proportional to the absorbance intensity, we concluded that the presence of graphene slightly decreased the amount of AgNPs in the Ag/PVA/Gr colloid dispersion (absorbance peak for Ag/PVA was 0.48 a.u., compared to the peak for Ag/PVA/Gr of 0.39 a.u.).

Transmission electron microscopy

From TEM micrographs depicted in Fig. 2 (a), (b) and (c) it is obvious that the AgNPs assume sphere-like morphologies in appearance at nanoscale levels of approximately 10-40 nm in diameter for both Ag/PVA (Fig. 2a,b) and Ag/PVA/Gr (Fig. 2c). However, at lower current

density of 15 mA cm^{-2} (Fig. 2a) silver nanoparticles exhibit greater tendency for aggregation and agglomeration than at higher current density, 40 mA cm^{-2} (Fig. 2b), confirming the optimal value of current density of 40 mA cm^{-2} . Fig. 2c shows TEM micrograph of Ag/PVA/Gr colloid dispersion at 40 mA cm^{-2} ($t_{\text{synt.}} = 30 \text{ min}$), proving also that presence of graphene slightly decreased the amount of AgNPs in respect to Ag/PVA dispersion.

and time of synthesis 10 min, and (b) variable time of synthesis at current density of 40 mA cm^{-2} .

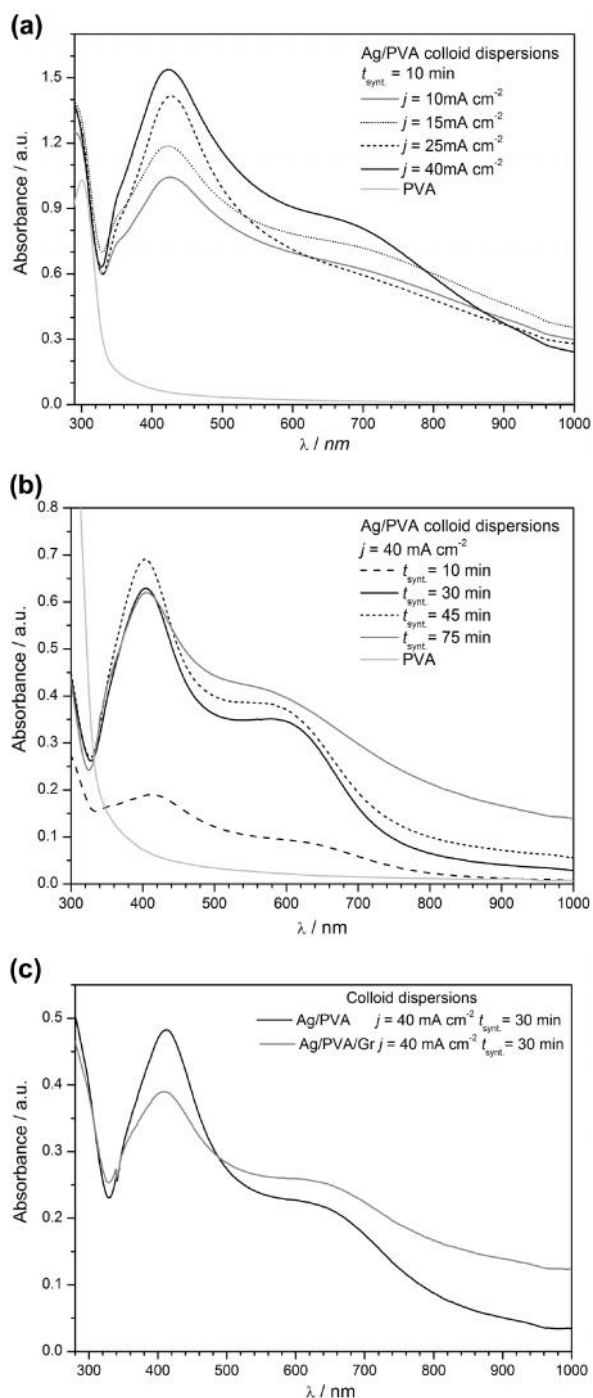


Fig. 1. UV-Vis spectra of PVA solution and electrochemically synthesized silver nanoparticles in Ag/PVA colloid dispersions: (a) variable current density

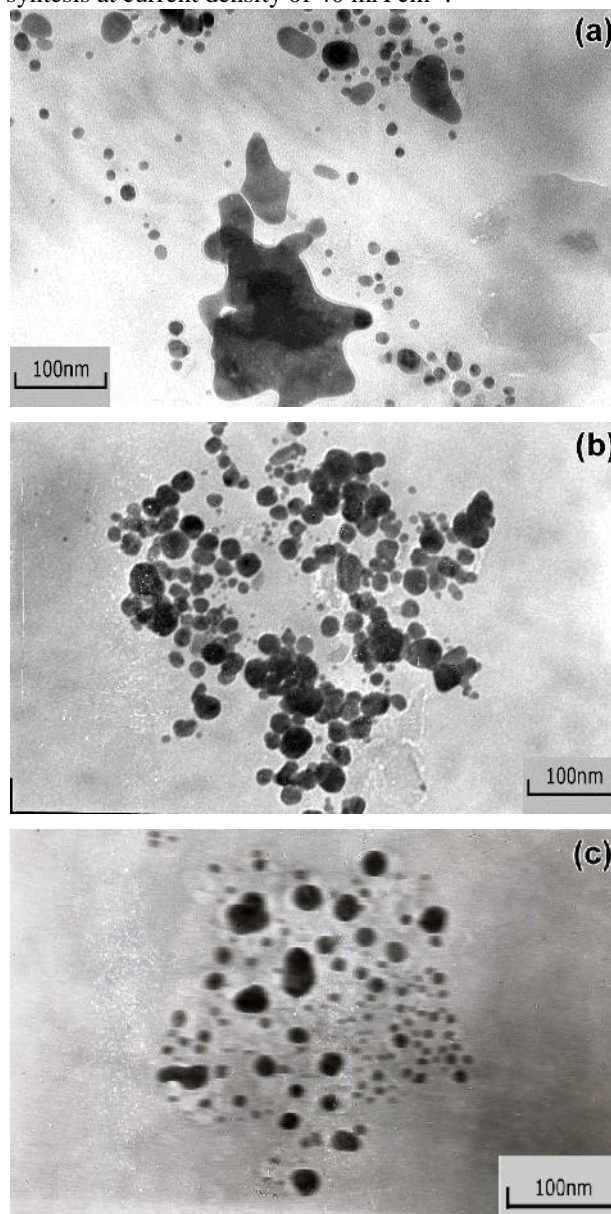


Fig. 2. TEM micrographs of electrochemically synthesized silver nanoparticles in Ag/PVA colloid dispersion ($t_{\text{synt.}} = 10 \text{ min}$) at different values of current density: (a) 15 mA cm^{-2} , (b) 40 mA cm^{-2} and (c) Ag/PVA/Gr colloid dispersion at 40 mA cm^{-2} ($t_{\text{synt.}} = 30 \text{ min}$).

Cyclic voltammetry

The cyclic voltammetry of Pt electrode analysis was performed in 10 wt% PVA solution and in colloid dispersion of Ag/PVA (Fig. 3) obtained at different values of current density, 25 and 40 mA cm^{-2} , for 10 min of synthesis time. A better insight into the oxidation/reduction processes occurring in aqueous solutions of silver was obtained by the comparison with cyclic voltammograms of Pt electrode in solutions containing 3.9 mM AgNO_3 and 0.1 M KNO_3 .

Cyclic voltammogram of Pt electrode in 10 wt% PVA solution (Fig. 3) exhibited a broad cathodic peak at -100 mV, originating from Pt oxide reduction formed during the anodic sweep. The anodic counterpart of this peak is not seen due to the overlapping with the oxidation current at potentials more positive than 400 mV.

Stationary cyclic voltammograms of Pt electrode in both Ag/PVA colloid dispersions exhibited three anodic peaks at around 595 mV, 665 mV, 875 mV for current density of 25 mA cm⁻² and 560 mV, 700 mV, 880 mV for current density of 40 mA cm⁻² (Fig. 3) The first two can be related to the different oxidation processes of silver nanoparticles in the Ag/PVA colloid solutions, while the peaks at around 875 and 880 mV are related to the Pt oxide. Only one cathodic peak was observed at around 165 mV and 135 mV, for 25 mA cm⁻² and 40 mA cm⁻², respectively. Two anodic peaks suggest there is a difference between silver species; one is even less susceptible for oxidation. This could be explained by the entrapment of silver nanoparticles by PVA molecules, which implies that enhanced stability of silver nanoparticles was obtained. The results indicated two types of AgNPs in Ag/PVA colloid solution coexisted; the relatively free ones that are susceptible to the oxidation, and those already bonded to PVA molecules, and hence less reactive.

The cyclic voltammogram of Pt electrode in Ag/PVA/Gr colloid dispersion [18] revealed two anodic peaks, one at around 650 mV due to AgNPs oxidation, and the second at around 950 mV due to oxidation of free Pt surfaces and Pt oxide formation. Two cathodic counterparts were observed: a peak at around 130 mV corresponding to AgNP reduction and a peak at around -370 mV due to reduction of the Pt oxide.

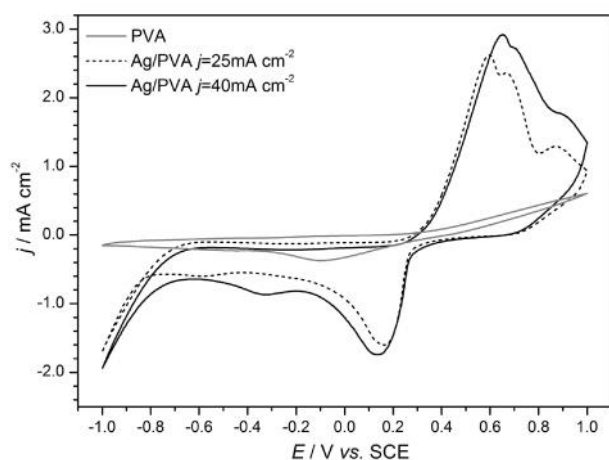


Fig. 3. Stationary cyclic voltammograms for Pt electrode in PVA solution and Ag/PVA colloid dispersions ($j = 25 \text{ mA cm}^{-2}$ and $j = 40 \text{ mA cm}^{-2}$, $t_{\text{synt.}} = 10 \text{ min}$).

Fourier transform infrared (FT-IR) and Raman spectroscopy

FT-IR measurements were performed on pure PVA, Ag/PVA and Ag/PVA/Gr thin films in order to determine the type of interactions between PVA molecules, silver nanoparticles and graphene. Thin films were obtained by solvent evaporation from PVA solution and Ag/PVA colloid dispersion (Fig. 4, Table 1) and Ag/PVA/Gr colloid dispersions [18]. The spectrum of the pure PVA film exhibited characteristic peaks associated with poly(vinyl alcohol). A typical strong hydroxyl band for -OH stretching vibration was observed at 3252 cm⁻¹ [32]; absorption peak originating from carboxyl stretching band (C=O) was verified at a wavenumber of 1714 cm⁻¹. Vibration band in the region between 1090 and 1150 cm⁻¹ is attributed to the crystallinity of the PVA [33], considering that the PVA is a semi-crystalline synthetic polymer [34].

The FT-IR spectrum of Ag/PVA film (Fig. 4) and Ag/PVA/Gr film [18] exhibited few differences in comparison to the spectrum of the pure PVA. Important changes were observed for the band peaking at 1413 cm⁻¹ (PVA spectrum) compared to 1367 cm⁻¹, 1371 cm⁻¹ and 1353 cm⁻¹ (Ag/PVA spectrum for current density 15 mA cm⁻² and 40 mA cm⁻² at $t_{\text{synt.}} = 10 \text{ min}$, and Ag/PVA/Gr spectrum for current density 40 mA cm⁻² at $t_{\text{synt.}} = 30 \text{ min}$, respectively). The band peaking at 1325 cm⁻¹ disappeared upon incorporation of Ag nanoparticles, which suggested interaction between AgNPs and -OH groups originating from PVA molecules and graphene through the decoupling between the corresponding vibrations.

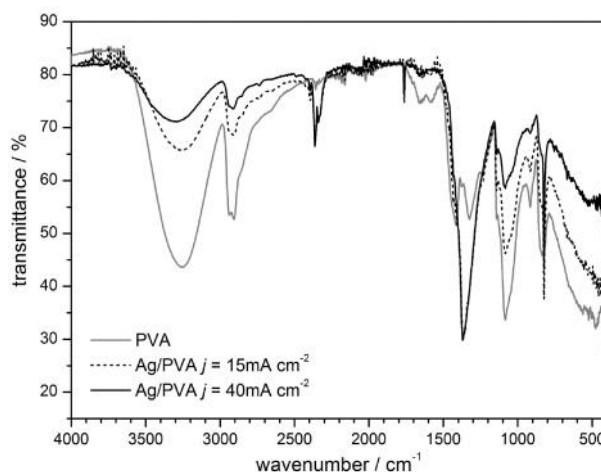


Fig. 4. FT-IR spectra of PVA and Ag/PVA thin films obtained by solvent evaporation from PVA solution and Ag/PVA colloid dispersions ($j = 15 \text{ mA cm}^{-2}$ and 40 mA cm^{-2} , $t_{\text{synt.}} = 10 \text{ min}$).

Table 1. Wavenumbers of the characteristic bands and corresponding assignments for PVA, Ag/PVA and Ag/PVA/Gr films.

PVA	Wavenumber/cm ⁻¹			Assignment [32-35]
	Ag/PVA 15 mA cm ⁻²	Ag/PVA 40 mA cm ⁻²	Ag/PVA/Gr 40 mA cm ⁻² [18]	
3252	3249	3288	3231	-OH stretching vibration
2908	2910	2940	2908	asymmetric CH ₂ stretching and aliphatic C-H stretching vibrations
1581			1578	C=C vibration stretching
1413 1325	1367	1371	1353	-OH in plane coupling with C-H wagging
1141	1142	1142	1139	symmetric C-C stretching
1082	1084	1084	1084	C-O stretching vibration of secondary alcohols
916	916	916	916	symmetric C-C stretching
833	823	823	833	C-H rocking vibration

In order to verify the incorporation of graphene in Ag/PVA/Gr composite hydrogel, Raman analysis was performed [18,19]. The presence of exfoliated graphene sheets embedded in the hydrogel matrix was confirmed by the broad spectral bands at 1379 cm⁻¹ (D-peak) and 1618 cm⁻¹ (G-peak) supporting our previously published results. The G-peak appears in the spectrum due to the graphitic structure of the material, whereas the D-peak reveals disordered structure of the carbon. Raman analysis confirmed graphene structure in its pure form [36-38].

Antibacterial agar diffusion test and silver release monitoring

Antibacterial activity of the samples was tested for microorganisms that are responsible for most of the inter-hospital infections, *S. aureus* and *E. coli*. The results of qualitative antimicrobial agar diffusion tests showed that both Ag/PVA and Ag/PVA/Gr successfully affect both microorganisms. The average inhibition zone was 0.4 mm for *S. aureus* and it can be easily observed around the sample disc of Ag/PVA/Gr and a bit less pronounced zone of 0.2 mm around the disc of Ag/PVA (Fig. 5). In the case of *E. coli* the average inhibition zone is much less pronounced, only 0.1 mm for both discs, Ag/PVA and Ag/PVA/Gr.

Quantitative results of antibacterial activity were obtained from test in suspension (phosphate buffer (PB)) using the spread plate method [18]. Both Ag/PVA and Ag/PVA/Gr hydrogels significantly reduced bacterial cell viability after just 1 h of incubation when compared to the initial number of

cells in suspension. Ag/PVA killed all the *S. aureus* colonies after 24 h and all the *E. coli* colonies after 3 h. In contrast, Ag/PVA/Gr completely destroyed all *S. aureus* TL and *E. coli* colonies after 3 h and 24 h, respectively. The greater antibacterial activity of Ag/PVA/Gr than Ag/PVA could be a consequence of the smaller dimensions of the AgNPs embedded in the hydrogel matrix, as discussed earlier.

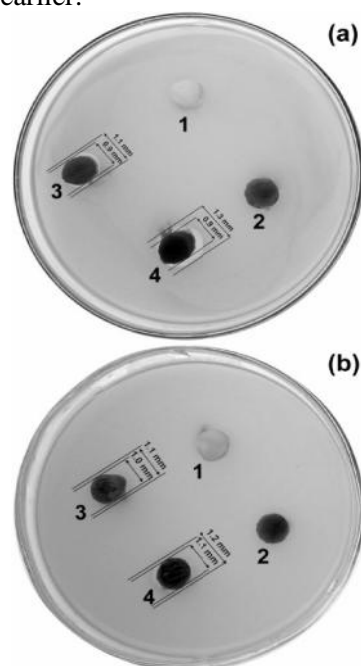


Fig. 5. Antibacterial activity of PVA (1), PVA/Gr (2), Ag/PVA (3) and Ag/PVA/Gr (4) hydrogels against strain (a) *S. aureus* and (b) *E. coli* by agar diffusion tests.

Also, antibacterial activity of graphene [39-41] contributes to better activity of Ag/PVA/Gr than

Ag/PVA hydrogel. Based on our results, it can be considered that both composites, Ag/PVA and Ag/PVA/Gr prevent biofilm formation [18].

The silver release kinetics from Ag/PVA and Ag/PVA/Gr hydrogel discs during time of exposure to SBF at 37 °C is depicted in Table 2.

Table 2. Time dependence of the concentration of silver released from Ag/PVA and Ag/PVA/Gr hydrogel discs (data represent average of three measurements).

Time/ days	Released silver from Ag/PVA hydrogel disc (wt. %)	Released silver from Ag/PVA/Gr hydrogel disc (wt.%)
1	14.1	17.1
2	15.7	18.5
3	16.3	19.1
4	17.0	19.7
5	17.6	20.2
6	18.1	20.7
7	18.6	21.1
10	19.4	21.7
14	20.6	22.5
24	22.4	23.2
28	23.5	23.9

The amount of silver released from a hydrogel was monitored as a function of time. It can be observed that the silver concentration released from Ag/PVA and Ag/PVA/Gr hydrogels initially increased swiftly with time, and after 3 days of silver release (16 wt. % and 19 wt. % of the initial silver content, respectively) a plateau was observed, indicating the significant lowering of the silver release rate. However, it can also be seen that even after 28 days, both Ag/PVA and Ag/PVA/Gr had released ~24 wt. % of the initial silver content, as a consequence of stability of AgNPs inside the highly crosslinked PVA hydrogel network [18]. This is very important since the remaining silver can preserve the sterility of the samples over time. As a result, these hydrogels could be used for a prolongation the sterility of a soft tissue implant for example.

CONCLUSIONS

In this work, Ag/PVA colloid dispersions were successfully obtained at different values of current density 10, 15, 25, 40 mA cm⁻² and different times of synthesis 10, 30, 45, 75 min. UV-Vis spectroscopy demonstrated that optimal synthesis parameters were- current density of 40 mA cm⁻² and time of 30 min. Comparison between Ag/PVA colloid dispersion synthesized at optimal conditions

with the Ag/PVA/Gr colloid dispersion synthesized at the same conditions, demonstrated that AgNPs in Ag/PVA/Gr nanocomposite had smaller dimensions than those in Ag/PVA nanocomposite due to the presence of graphene sheets between PVA chains. In addition, the interactions between AgNPs and hydroxyl groups in PVA, as well as between PVA and graphene sheets, were confirmed. Slow silver release (~24 wt. %) after 28 days in simulated body fluid confirmed that both Ag/PVA/Gr and Ag/PVA hydrogels can preserve sterility over time. This characteristic, combined with their strong antibacterial activity indicates that Ag/PVA/Gr and Ag/PVA hydrogels are excellent candidates for soft tissue implants and wound dressings.

Acknowledgements. This work was supported by the Basic Science Research Program through the National Research Foundation of Korea (NRF) funded by the Ministry of Education, Science and Technology (project number: 2016R1A2B4016034). The authors would like to express their gratitude to the Ministry of Education, Science and Technological Development, Republic of Serbia (Grant No. III 45019) for the financial support.

REFERENCES

1. S. Sasaki, T. Murakami, A. Suzuki, *Biosurf. Biotribol.*, **2**, 11 (2016).
2. J. H. Kim, H. Lee, A. W. Jatoi, S. S. Im, J. S. Lee, I.-S. Kim, *Mater. Lett.*, **181**, 367 (2016).
3. L. Fan, H. Yang, J. Yang, M. Peng, J. Hu, *Carbohydr. Polym.*, **146**, 427 (2016).
4. N. Georgieva, R. Bryaskova, R. Tzoneva, *Mater. Lett.*, **88**, 19 (2012).
5. J. Shen, D. J. Burgess, *Int. J. Pharm.*, **422**, 341 (2012).
6. J. L. Drury, D. J. Mooney, *Biomaterials*, **24**, 4337 (2003).
7. R. Ma, D. Xiong, F. Miao, J. Zhang, Y. Peng, *Mater. Sci. Eng., C*, **29**, 1979 (2009).
8. B. Bolto, T. Tran, M. Hoang, Z. Xie, *Prog. Polym. Sci.*, **34**, 969 (2009).
9. C. Cencetti, D. Bellini, A. Pavesio, D. Senigaglia, C. Passariello, A. Virga, P. Matricardi, *Carbohydr. Polym.*, **90**, 1362 (2012).
10. M.-Y. Lim, H. Shin, D. M. Shin, S.-S. Lee, J.-C. Lee, *Polymer*, **84**, 89 (2016).
11. A. Jankovi, S. Erakovi, M. Vukašinovi -Sekuli, V. Miškovi -Stankovi, S. J. Park, K. Y. Rhee, *Prog. Org. Coat.*, **83**, 1 (2015).
12. T. Zhou, F. Chen, C. Tang, H. Bai, Q. Zhang, H. Deng, Q. Fu, *Compos. Sci. Technol.*, **71**, 1266 (2011).
13. A. Jankovi, S. Erakovi, M. Mitri, I. Z. Mati, Z. D. Jurani, G. C. P. Tsui, C.-y. Tang, V. Miškovi -Stankovi, K. Y. Rhee, S. J. Park, *J. Alloys Compd.*, **624**, 148 (2015).
14. S. Bai, X. Shen, *RSC Advances*, **2**, 64 (2012).
15. X. Liu, W. Kuang, B. Guo, *Polymer*, **56**, 553 (2015).

